Available online at www.sciencedirect.com
ScienceDirect
Journal of Molecular Catalysis A: Chemical 261 (2007) 293–300
JOURNAL OF MOLECULAR CATALYSIS A: CHEMICAL
www.elsevier.com/locate/molcata

# Iron-based ethylene polymerization catalysts supported by bis(imino)pyridine ligands: Derivatization via deprotonation/alkylation at the ketimine methyl position

Stuart McTavish, George J.P. Britovsek, Theo M. Smit, Vernon C. Gibson *, Andrew J.P. White, David J. Williams

*Department of Chemistry, Imperial College London, South Kensington, London SW7 2AZ, UK*

Received 3 July 2006; received in revised form 12 October 2006; accepted 16 October 2006
Available online 21 October 2006

**Abstract**

Bis(imino)pyridine ligands, L [where L = 2,6-(ArNCR$^1$)$_2$C$_5$H$_3$N R$^1$ = Et, $^i$Pr, $CH_2CH_2Ph$ or $CH(CH_2Ph)_2$ and Ar = 2,4,6-(Me)$_3$C$_6$H$_2$ (MES) or 2,6-($^i$Pr)$_2$C$_6$H$_3$ (DIPP)] have been prepared by deprotonation of the parent ketimine ligand (R$^1$ = Me) using lithium diisopropylamide (LDA), followed by alkylation with the appropriate alkylhalide. The corresponding iron dichloride complexes $LFeCl_2$ are highly active ethylene polymerisation catalysts upon treatment with methylaluminoxane (MAO), with activities in the range of 3000–18,000 g/mmol bar h. The molecular weights ($M_n$) of the resultant polyethylenes lie in the range of 6500–24,000 with broad molecular weight distributions (16.5–38.0). The nature of the imine carbon substituent has a marked effect on the polymer molecular weight whereas the catalyst activity is largely unaffected by changes to this substituent.


*Keywords:* Iron; Ethylene; Imine; Polymerization; Pyridine

## 1. Introduction

Since the first reports of active ethylene polymerization catalysts based on iron and cobalt supported by bis(imino)pyridine ligands [1–3] there have been numerous studies directed at modifying the bis(imino)pyridine frame [1,4–21] especially the groups attached to the imine nitrogen donors [4–13]. Relatively little attention has been directed towards changes to the substituents at the imine carbon atoms. Bennett and co-workers reported an imidazolyl substituted derivative that showed similar activity to its ketimine analogue [14]. Recently, we described the synthesis, characterization and polymerization behavior of catalysts containing ether and thioether functionalities attached to the imine carbon atom [15]. Here, we describe a straightforward deprotonation/alkylation procedure that allows systematic variations at the imine carbon position. A related approach has been utilized to prepare alkenyl-functionalized bis(imino)pyridine iron complexes [16].

## 2. Experimental section

### 2.1. General

All manipulations were carried out under an atmosphere of nitrogen using standard Schlenk and cannula techniques or in a conventional nitrogen-filled glovebox. Solvents were refluxed over an appropriate drying agent, and distilled and degassed prior to use. Elemental analyses were performed by the microanalytical services of University College London, Department of Chemistry and Mikroanalytisches Labor Pascher. NMR spectra were recorded on a Bruker spectrometer at 250 MHz ($^1$H) and 62.9 MHz ($^{13}$C) at 293 K; chemical shifts are referenced to the residual protio impurity of the deuterated solvent. Mass spectra were obtained using either fast atom bombardment (FAB) or chemical ionization (CI). IR spectra were recorded on a Perkin-Elmer Spectrum GXI instrument. Magnetic moments

* Corresponding author.
*E-mail address:* v.gibson@imperial.ac.uk (V.C. Gibson).

1381-1169/$ – see front matter © 2006 Elsevier B.V. All rights reserved.
doi:10.1016/j.molcata.2006.10.028

were obtained by the Evans' NMR method (solvent, $CH_2Cl_2$; reference cyclohexane) [22]. Polymer GPC analyses were carried out at BP Chemicals, Ltd. on a Waters 150CV (columns supplied by Shodex (807, 806 and 804)) using polyethylene standard reference material NBS1484a. Lithium diisopropylamide [23] and 2,6-diacetylpyridinebis(2,4,6-trimethylanil)iron dichloride (**7b**) [1] were prepared according to literature procedures. *n*-Butyllithium was purchased from Fisher Scientific UK. Research grade ethylene (BOC, Grade 3.50) was used for all ethylene polymerisation experiments.

### 2.2. Synthesis of preligands *1a–6a* and complexes *1b–6b*

#### 2.2.1. Preparation of {2,6-[(2,4,6-(Me)$_3$C$_6$H$_2$)NCCH$_2$CH$_3$]$_2$C$_5$H$_3$N} (*1a*)

Lithium diisopropylamide [2.2 equiv., 2.77 mmol; freshly prepared from diisopropylamine (0.39 ml, 2.77 mmol) and *n*-butyllithium (1.73 ml, 2.77 mmol, 1.6 M in hexanes) in THF (5 ml)] was added dropwise to a solution of 2,6-diacetylpyridinebis(2,4,6-trimethylanil) (0.50 g, 1.26 mmol) in THF (30 ml) at −78 °C. The resulting dark solution was allowed to warm to 0 °C with stirring (2 h). Iodomethane (0.17 ml, 2.77 mmol, 2.2 equiv.) was then added and the ensuing solution was allowed to warm to room temperature (12 h) to form a yellow solution. The solvent was removed under reduced pressure and the residue was dissolved in 40 ml of diethylether. The solution was washed with water (3 × 30 ml) and the organic phase was dried over $MgSO_4$. The volatile components were removed under reduced pressure and the residue was recrystallised from ethanol to yield **1a** as a yellow solid (0.52 g, 98%). $^1$H NMR ($CDCl_3$): $\delta$ 8.42 (d, 2H, $^3J$(HH) 7.9, Py-$H_m$), 7.91 (t, 1H, Py-$H_p$), 6.91 (s, 4H, Ar-*H*), 2.72 (q, 4H, $^3J$(HH) 7.5, N=CC$H_2$CH$_3$), 2.31 (s, 6H, C*Me*), 2.05 (s, 12H, C*Me*), 1.04 (t, 6H, N=CCH$_2$C$H_3$). $^{13}$C NMR (CDCl3, {$^1$H}): $\delta$ 171.71 (N=*C*), 154.56 (Py-*C*o), 145.92 (Ar-*C*ip), 136.98 (Ar-*C*o), 132.08 (Ar-*C*p), 128.57 (Py-*C*p), 125.17 (Py-*C*m), 122.85 (Ar-*C*m), 23.14 (N=C–*C*H$_2$CH$_3$), 20.73 (Ar-*Me*$_p$), 18.08 (Ar-*Me*o), 11.30 (N=C–CH$_2$*C*H$_3$). MS (CI), *m/z* 426 [(*M* + H)$^+$]. IR $\nu_{(C=N)}$ 1634 (s), 1567 (s) cm$^{-1}$. Anal. ($C_{29}H_{35}N_3$·0.25$H_2O$) calcd.: C, 80.98; H, 8.32; N, 9.77; found, C, 80.92; H, 7.99; N, 9.32.

#### 2.2.2. Preparation of {2,6-[(2,4,6-(Me)$_3$C$_6$H$_2$)NCCH(Me)$_2$]$_2$C$_5$H$_3$N} (*2a*)

Procedure as described for **1a**, but employing **1a** to give **2a** as a yellow powder in 72% yield. $^1$H NMR ($CDCl_3$): $\delta$ 8.02 (broad, d, $^3J$(HH) 7.8 2H, Py-$H_m$), 6.86, and 6.66 (broad, m, 4H, Ar-*H*), 6.39 (broad, m, 1H, Py-$H_p$), 3.76, 3.50 and 2.91 (broad, 2H, C*H*Me$_2$), 2.22 (broad, m, 6H, Ar-C*Me*p), 2.05 (broad, m, 12H, Ar-CMeo), 1.45 and 1.36 (broad, m, 12H, CH*Me*$_2$). $^{13}$C NMR (CDCl3, {$^1$H}): $\delta$ 172.62, 172.13 and 171.62 (N=C), 153.05 (Py-*C*o), 145.57, 144.92 and 144.50 (Ar-*C*ip), 137.62, 136.21 and 136.16 (Ar-*C*o), 132.56 (Ar-*C*p), 128.61 (Py-*C*p), 125.98 (Py-*C*m), 123.15, 123.08 and 122.93 (Ar-*C*m), 35.60, 34.79 and 34.30 (N=C–*C*H(Me)$_2$), 23.78, 23.58 and 23.56 (N=C–CH(*Me*)$_2$), 20.61 (Ar–*Me*p), 18.48, 18.27 and 18.20 (Ar–*Me*o). MS (CI), *m/z* 454 [(*M* + H)$^+$]. IR $\nu_{(C=N)}$ 1651 (s), 1567 (s) cm$^{-1}$. Anal. ($C_{31}H_{39}N_3$·0.66$H_2O$) calcd.: C, 79.98; H, 8.73; N, 9.03; found, C, 79.97; H, 8.68; N, 8.77.

#### 2.2.3. Preparation of {2,6-[(2,4,6-(Me)$_3$C$_6$H$_2$)NCCH$_2$CH$_2$C$_6$H$_5$]$_2$C$_5$H$_3$N} (*3a*)

Lithium diisopropylamide [2.2 equiv., 5.54 mmol; freshly prepared from diisopropylamine (0.78 ml, 5.53 mmol) and *n*-butyllithium (3.46 ml, 5.53 mmol, 1.6 M in hexanes) in THF (8 ml)] was added dropwise to a solution of 2,6-diacetylpyridinebis(2,4,6-trimethylanil) (1.00 g, 2.52 mmol) in THF (50 ml) at −78 °C. The resulting dark solution was allowed to warm to 0 °C with stirring (2 h). Benzylbromide (0.72 ml, 6.04 mmol, 2.4 equiv.) was then added and the ensuing solution was allowed to warm to room temperature (12 h) to give a yellow solution. The solvent was removed under reduced pressure and the residue was dissolved in 40 ml of diethylether. The solution was then washed with water (3× 30 ml) and the organic phase dried over $MgSO_4$. The volatile components were removed under reduced pressure and the residue was recrystallised from ethanol to yield **3a** as a yellow solid (0.88 g, 61 %). $^1$H NMR ($CDCl_3$): $\delta$ 8.45 (d, 2H, $^3J$(HH) 7.9, Py-$H_m$), 7.97 (t, 1H, Py-$H_p$), 6.90 (s, 4H, Ar-*H*), 7.26–6.83 (m, 10H, N=CCH$_2$CH$_2$*Ph*), 3.06 (m, 4H, N=CC$H_2$CH$_2$Ph), 2.78 (m, 4H, N=CCH$_2$C$H_2$Ph), 2.31 (s, 6H, Ar-C*Me*), 2.03 (s, 12H, Ar-C*Me*). $^{13}$C NMR (CDCl3, {$^1$H}): $\delta$ 169.83 (N=*C*), 154.93 (Py-*C*o), 145.60 (Ar-*C*ip), 141.02 (Ph-*C*ip), 137.27 (Ar-*C*o), 132.33 (Ar-*C*p), 128.85 (Ph-*C*o), 128.36 (Ph-*C*p), 128.12 (Ph-*C*m), 126.00 (Py-*C*p), 125.12 (Py-*C*m), 122.76 (Ar-*C*m), 32.80 (N=C-*C*H$_2$CH$_2$Ph), 20.76 (Ar-*Me*$_p$), 18.09 (Ar-*Me*$_o$), 31.75 (N=C-CH$_2$*C*H$_2$Ph). MS (CI), *m/z* 578 [(*M* + H)$^+$]. IR $\nu_{(C=N)}$ 1638 (s), 1567 (s) cm$^{-1}$. Anal. ($C_{39}H_{43}N_3$) calcd.: C, 84.57; H, 7.53; N, 7.22; found, C, 84.56; H, 7.47; N, 7.29.

#### 2.2.4. Preparation of {2,6-[(2,4,6-(Me)$_3$C$_6$H$_2$)NCCH(CH$_2$C$_6$H$_5$)$_2$]$_2$C$_5$H$_3$N} (*4a*)

Procedure as described for **3a**, but employing **3a** to give **4a** as a viscous yellow oil in 58 % yield. $^1$H NMR ($CDCl_3$): $\delta$ 8.50 (broad, 2H, Py-$H_m$), 8.0 (broad, 1H, Py-$H_p$), 6.88 (broad, m, 4H, Ar-*H*), 7.15–6.87 (broad, m, 20H, N=CCH(CH$_2$*Ph*)$_2$), 3.45 (broad, 2H, N=CC*H*(CH$_2$Ph)$_2$), 2.91 (broad, m, 8H, N=CCH(C$H_2$Ph)$_2$), 2.34 (broad, m, 6H, C*Me*), 2.05 (broad, m, 12H, C*Me*). MS (CI), *m/z* 758 [(*M* + H)$^+$]. Pre-ligand **4a** is a highly viscous compound and satisfactory elemental analysis could not be obtained.

#### 2.2.5. Preparation of {2,6-[(2,6-(CH(Me)$_2$)$_2$C$_6$H$_3$)NCCH$_2$CH$_3$]$_2$C$_5$H$_3$N} (*5a*)

Procedure as described for **1a** using 2,6-diacetylpyridinebis(2,6-diisopropylanil) to give **5a** as a yellow powder in 96% yield. $^1$H NMR ($CDCl_3$): $\delta$ 8.40 (d, 2H, $^3J$(HH) 7.8, Py-$H_m$), 7.93 (t, 1H, Py-$H_p$), 7.1 (m, 6H, Ar-*H*), 2.84–2.69 (m, 8H, C*H*Me$_2$ and N=CC$H_2$CH$_3$), 1.18 (d, 24H, CH*Me*$_2$), 1.08 (t, 6H, $^3J$(HH) 8.8, N=CCH$_2$C$H_3$). $^{13}$C NMR ($CDCl_3$, {$^1$H}): $\delta$ 170.61 (N=C), 154.48 (Py-C$_o$), 146.05 (Ar-$C_{ip}$), 137.44 (Ar-$C_o$), 137.09 (Ar-$C_p$), 135.61 (Py-$C_p$), 123.45 (Py-$C_m$), 122.83 (Ar-$C_m$), 28.28 (CH*Me*$_2$), 23.61 (N=C–*C*H$_2$CH$_3$),

22.23 (*C*HMe$_2$), 11.01 (N=C–CH$_2$*C*H$_3$). MS (CI), *m/z* 510 [$(M+H)^+$]. IR $\nu_{(C=N)}$ 1637 (s), 1570 (s) cm$^{-1}$. Anal. ($C_{35}H_{47}N_3$) calcd.: C, 82.46; H, 9.29; N, 8.24; found, C, 82.11; H, 9.22; N, 8.17.

### 2.2.6. Preparation of {2,6-[(2,6-(CH(Me)$_2$)$_2$C$_6$H$_3$)NCCH(Me)$_2$]$_2$C$_5$H$_3$N} (**6a**)

Procedure as described for **1a** using **5a** to give **6a** as a yellow powder in 70% yield. $^1$H NMR ($CDCl_3$): $\delta$ 8.00 (broad, m, 2H, Py-*H*$_m$), 7.99 (broad, m, 1H, Py-*H*$_p$), 7.15 (broad, m, 6H, Ar-*H*), 2.78 (broad, m, 6H, C*H*Me$_2$), 1.40–0.91 (m, 36H, CH(*Me*)$_2$). $^{13}$C NMR ($CDCl_3$, {$^1$H}): $\delta$ 172.67 and 171.61 (N=C), 156.20 (Py-C$_o$), 153.28 and 152.32 (Ar-*C*$_{ip}$), 145.78 (Ar-*C*$_o$), 135.60 (Ar-*C*$_p$), 135.29 (Py-*C*$_p$), 123.46 (Py-*C*$_m$), 123.15 and 122.78 (Ar-*C*$_m$), 35.11 and 32.24 (N=C–*C*H(Me)$_2$), 28.26 and 28.03 (Ar-CH*Me*$_2$), 23.43 and 22.13 (Ar-*C*HMe$_2$), 20.59 and 19.64 (N=C–CH(*Me*)$_2$). MS (CI), *m/z* 538 [$(M+H)^+$]. IR $\nu_{(C=N)}$ 1645 (s), 1567 (s) cm$^{-1}$. Anal. ($C_{37}H_{51}N_3$) calcd.: C, 82.63; H, 9.56; N, 7.81; found, C, 81.98; H, 9.69; N, 7.80.

### 2.2.7. Preparation of {2,6-[(2,4,6-(Me)$_3$C$_6$H$_2$)NCCH$_2$CH$_3$]$_2$C$_5$H$_3$N}FeCl$_2$ (**1b**)

A suspension of **1a** (0.275 g, 0.647 mmol) in *n*-butanol was added dropwise at 80 °C to a solution of $FeCl_2$ (1 equiv., 0.082 g, 0.647 mmol) in *n*-butanol (20 ml) to yield a blue solution. After stirring at 80 °C for 12 h, the reaction was allowed to cool to room temperature. The reaction volume was concentrated and diethylether (30 ml) was added to precipitate the product as a blue powder. The powder was subsequently washed with diethylether (3× 10 ml) and dried under reduced pressure to yield 0.31 g (87%) of **1b**. $^1$H NMR ($CD_2Cl_2$, broad singlets are observed in each case): $\delta$ 84.8 (2H, Py-*H*$_m$), 44.5 (1H, Py-*H*$_p$), 23.1 (6H, Ar-*Me*$_p$), 15.5 (4H, Ar-*H*$_m$), 12.5 (12H, Ar-*Me*$_o$), 6.6 (4H, N=CC*H*$_2$CH$_3$). −5.5 (6H, N=CCH$_2$C*H*$_3$). MS (FAB) *m/z* 551 [$M^+$], 516 [$M^+$ − Cl], 481 [$M^+$ − 2Cl]. Anal. $C_{29}H_{35}N_3FeCl_2\cdot0.5H_2O$ calcd.: C, 61.07; H, 6.54; N, 7.36; found, C, 61.37; H, 6.43; N, 6.69. $\mu_{eff}$ (Evans' NMR Method) 5.09 BM.

### 2.2.8. Preparation of {2,6-[(2,4,6-(Me)$_3$C$_6$H$_2$)NCCH(Me)$_2$]$_2$C$_5$H$_3$N}FeCl$_2$ (**2b**)

Procedure as described for **1b** using **2a** and $FeCl_2$ to give **2b** as a blue powder in 94% yield. $^1$H NMR ($CD_2Cl_2$, broad singlets are observed in each case): $\delta$ 86.5 (2H, Py-*H*$_m$), 54.8 (1H, Py-*H*$_p$), 24.6 (6H, Ar-*Me*$_p$), 20.3 (4H, Ar-*H*m), 15.6 (2H, N=CC*H*(Me)$_2$), 10.8 (12H, Ar-*Me*o), −3.7 (12H, N=CCH(Me)$_2$). MS (FAB), *m/z* 579 [$M^+$], 544 [$M^+$-Cl], 509 [$M^+$ − 2Cl]. Anal. $C_{31}H_{39}N_3FeCl_2\cdot0.5H_2O$ calcd.: C, 63.17; H, 6.84; N, 7.13; found, C, 63.01; H, 7.37; N, 6.25. $\mu_{eff}$ (Evans' NMR Method) 5.03 BM.

### 2.2.9. Preparation of {2,6-[(2,4,6-(Me)$_3$C$_6$H$_2$)NCCH$_2$CH$_2$C$_6$H$_5$]$_2$C$_5$H$_3$N}FeCl$_2$ (**3b**)

Procedure as described for **1b** using **3a** and $FeCl_2$ to give **3b** as a blue powder in 79% yield. $^1$H NMR ($CD_2Cl_2$, broad singlets are observed in each case): $\delta$ 83.1 (2H, Py-*H*$_m$), 56.3 (1H, Py-*H*$_p$), 23.7 (6H, Ar-*Me*$_p$), 15.4 (4H, Ar-*H*$_m$), 12.7 (12H, Ar-*Me*$_o$), 6.5 (4H, N=CC*H*$_2$CH$_2$Ph), 5.4 (4H, N=CCH$_2$CH$_2$*Ph*), 5.3 (2H, N=CCH$_2$CH$_2$*Ph*), 4.4 (4H, N=CCH$_2$CH$_2$*Ph*), −2.4 (4H, N=CCH$_2$C*H*$_2$Ph). MS (FAB), *m/z* 703 [$M^+$], 668 [$M^+$ − Cl], 633 [$M^+$ − 2Cl]. Anal. ($C_{39}H_{43}N_3FeCl_2$) calcd.: C, 68.83; H, 6.37; N, 6.17; found, C, 68.73; H, 6.07; N, 5.72. $\mu$eff (Evans' NMR Method) 5.34 BM.

### 2.2.10. Preparation of {2,6-[(2,4,6-(Me)$_3$C$_6$H$_2$)NCCH(CH$_2$C$_6$H$_5$)$_2$]$_2$C$_5$H$_3$N}FeCl$_2$ (**4b**)

Procedure as described for **1b** using **4a** and $FeCl_2$ to give **4b** as a blue powder in 73% yield. $^1$H NMR ($CD_2Cl_2$, broad singlets are observed in each case): 87.3 (2H, Py-*H*$_m$), 72.6 (1H, Py-*H*$_p$), 25.7 (6H, Ar-*Me*$_p$), 24.7 (8H, N=CCH(C*H*$_2$Ph)$_2$), 18.0 (4H, Ar-*H*$_m$), 14.8 (12H, Ar-*Me*$_o$), 7.8 (2H, N=CC*H*(CH$_2$Ph)$_2$), 6.1 (8H, CH$_2$*Ph*), 5.3 (4H, CH$_2$*Ph*), 5.0 (8H, CH$_2$*Ph*). MS (FAB), *m/z* 883 [$M^+$], 848 [$M^+$ − Cl], 813 [$M^+$ − 2Cl]. Anal. ($C_{55}H_{55}N_3FeCl_2\cdot1.5H_2O$) calcd.: C, 72.45; H, 6.41; N, 4.61; found, C, 72.33; H, 5.85; N, 4.49. $\mu_{eff}$ (Evans' NMR Method) 5.00 BM.

### 2.2.11. Preparation of {2,6-[(2,6-(CH(Me)$_2$)$_2$C$_6$H$_3$)NCCH$_2$CH$_3$]$_2$C$_5$H$_3$N}FeCl$_2$ (**5b**)

Procedure as described for **1b** using **5a** and $FeCl_2$ to give **5b** as a blue powder in 74% yield. $^1$H NMR ($CD_2Cl_2$, broad singlets are observed in each case): $\delta$ 85.6 (1H, Py-*H*$_p$), 82.6 (2H, Py-*H*$_m$), 14.6 (4H, Ar-*H*$_m$), −0.7 (4H, N=CC*H*$_2$CH$_3$), −5.3 (12H, Ar-*i*-Pr-*Me*), −6.9 (12H, Ar-*i*-Pr-*Me*), −8.4 (6H, N=CCH$_2$(Me)$_2$), −10.9 (2H, Ar-*H*p), −26.8 (4H, Ar-*i*-Pr-C*H*). MS (FAB), *m/z* 635 [$M^+$], 600 [$M^+$ − Cl], 565 [$M^+$ − 2Cl]. Anal. ($C_{35}H_{47}N_3FeCl_2$) calcd.: C, 66.04; H, 7.44; N, 6.60; found, C, 65.73; H, 7.22; N, 6.45. $\mu_{eff}$ (Evans' NMR Method) 5.20 BM.

### 2.2.12. Preparation of {2,6-[(2,6-(CH(Me)$_2$)$_2$C$_6$H$_3$)NCCH(Me)$_2$]$_2$C$_5$H$_3$N}FeCl$_2$ (**6b**)

Procedure as described for **1b** using **6a** and $FeCl_2$ to give **6b** as a blue powder in 71% yield. $^1$H NMR ($CD_2Cl_2$, broad singlets are observed in each case): $\delta$ 88.3 (2H, Py-*H*m), 82.4 (1H, Py-*H*$_p$), 17.6 (2H, N=CC*H*(Me)$_2$), 14.1 (4H, Ar-*H*m), −5.4 (12H, Ar-*i*-Pr-*Me*), −6.3 (12H, Ar-*i*-Pr-*Me*), −3.2 (12H, N=CCH(Me)$_2$), −10.7 (2H, Ar-*H*p), −29.7 (4H, Ar-*i*-Pr-C*H*). MS (FAB), *m/z* 663 [$M^+$], 628 [$M^+$ − Cl], 593 [$M^+$ − 2Cl]. Anal. ($C_{37}H_{51}N_3FeCl_2$) calcd.: C, 66.87; H, 7.74; N, 6.32; found, C, 66.49; H, 7.43; N, 6.01. $\mu$eff (Evans' NMR Method) 5.12 BM.

## 2.3. X-ray crystallography

### 2.3.1. Crystal data for **1b**

$C_{29}H_{35}Cl_2FeN_3\cdot CH_2Cl_2$, $M$ = 637.28, orthorhombic, $Pna2_1$ (no. 33), $a$ = 17.7689(11), $b$ = 15.2630(6), $c$ = 23.8344(11) Å, $V$ = 6464.0(6) Å$^3$, $Z$ = 8 (two independent molecules), $D_c$ = 1.310 g cm$^{-3}$, $\mu$(Cu Kα) = 6.955 mm$^{-1}$, $T$ = 293 K, green platy needles; 5408 independent measured reflections, $F^2$ refinement, $R_1$ = 0.066, $wR_2$ = 0.133, 2986 independent observed absorption-corrected reflections [$|F_o| > 4\sigma(|F_o|)$, $2\theta_{max}$ = 128°], 765 parameters. The structure of **1b** was shown to be a polar twin by a combination of *R*-factor tests

[$R_1{}^+ = 0.0681$, $R_1{}^- = 0.0683$] and by use of the Flack parameter [$x^+ = +0.46(4)$, $x^- = +0.54(4)$] CCDC 606439.

### 2.3.2. Crystal data for **2b**

$C_{31}H_{39}Cl_2FeN_3{\cdot}CH_2Cl_2$, $M = 665.33$, triclinic, $P\bar{1}$ (no. 2), $a = 15.1126(9)$, $b = 15.7923(9)$, $c = 17.3838(14)$ Å, $\alpha = 69.152(6)$, $\beta = 69.167(7)$, $\gamma = 69.367(7)^\circ$, $V = 3500.5(4)$ Å$^3$, $Z = 4$ (two independent molecules), $D_c = 1.262$ g cm$^{-3}$, $\mu$(Cu-K$\alpha$) = 6.443 mm$^{-1}$, $T = 293$ K, dark blue prismatic needles; 10,196 independent measured reflections, $F^2$ refinement, $R_1 = 0.080$, $wR_2 = 0.198$, 6218 independent observed absorption-corrected reflections [$|F_o| > 4\sigma(|F_o|)$, $2\theta_{max} = 120^\circ$], 741 parameters. CCDC 606440.

### 2.3.3. Crystal data for **6b**

$C_{37}H_{51}Cl_2FeN_3$, $M = 664.56$, monoclinic, $Pn$ (no. 7), $a = 9.7637(6)$, $b = 12.8384(4)$, $c = 14.8855(13)$ Å, $\beta = 93.479(7)^\circ$, $V = 1862.5(2)$ Å$^3$, $Z = 2$, $D_c = 1.185$ g cm$^{-3}$, $\mu$(Cu-K$\alpha$) = 4.763 mm$^{-1}$, $T = 293$ K, blue platy needles; 2932 independent measured reflections, $F^2$ refinement, $R_1 = 0.046$, $wR_2 = 0.106$, 2507 independent observed absorption-corrected reflections [$|F_o| > 4\sigma(|F_o|)$, $2\theta_{max} = 128^\circ$], 389 parameters. The absolute structure of **6b** was determined by a combination of $R$-factor tests [$R_1{}^+ = 0.0457$, $R_1{}^- = 0.0743$] and by use of the Flack parameter [$x^+ = +0.017(13)$, $x^- = +0.983(13)$]. CCDC 606441.

### 2.4. Ethylene polymerisation procedure

A 1 l stainless steel reactor was heated under a nitrogen flow for 1 h at 85 °C and subsequently cooled to the temperature required for the polymerization run. Isobutane (0.5 l), an alkylaluminium scavenger (triisobutylaluminium, trimethylaluminium or MAO) and the desired pressure of ethylene were introduced into the reactor and the mixture was stirred at the polymerisation temperature for 30 min. A toluene solution of the catalyst was then injected under nitrogen. The reactor pressure was maintained constant throughout the polymerisation run (60 min.) by computer controlled addition of ethylene. Runs were terminated by venting off the volatile components. The reactor contents were isolated, washed with aqueous hydrogen chloride, methanol and then dried under vacuum at 50 °C.

## 3. Results and discussion

### 3.1. Synthesis and characterization

Ligands **1a**-**6a** were prepared by a straightforward protocol in which the methyl substituent of the α-imino carbon moiety in **I** or **II** is deprotonated using freshly prepared LDA at −78 °C, followed by alkylation using a primary alkylhalide at 0 °C (Scheme 1). This procedure can be repeated as necessary to build up the desired substitution pattern at the α-imino carbon position. Sequential deprotonation and alkylation of the imine functionality was found to be superior to analogous treatment of the ligand precursor, 2,6-diacetylpyridine. The latter route was also discounted on the grounds that an increased size of the carbonyl substituents in the ligand precursor would likely prove problematic in the subsequent amine condensation reactions. The effect of increasing the size of the imino alkyl substituent on the solution properties of **1a**–**6a** is apparent from their $^1$H NMR spectra. Thus, while the spectrum of **1a** is sharp at room temperature, the isopropyl derivative **2a** affords a broadened spectrum, consistent with restricted rotation. Similar broadening is also seen for **4a**, **5a** and **6a**.

2,6-Bis(imino)pyridyl iron(II) chloride pre-catalysts **1b**–**6b** can be synthesised in good yield by treatment of iron(II) chloride with the corresponding 2,6-bis(imino)pyridine ligand in *n*-butanol at elevated temperature. **1b**–**6b** are paramagnetic, with room temperature magnetic moments ($\mu_{eff}$) ranging from 5.0 to 5.5 BM (Evans' NMR method [22]), corresponding to four unpaired electrons and consistent with high spin iron(II) centres. Nevertheless, assignable contact-shifted $^1$H NMR spectra can be obtained (see Experimental).

### 3.2. Molecular structures of **1b**, **2b** and **6b**

The 2,6-bis(imino)pyridyl iron(II) chloride pre-catalysts have been shown to assume both square-based pyramidal and trigonal bipyramidal geometries depending upon the ligand substitution pattern of the aryl ring.[1] In order to further probe the geometries adopted by this class of complex, structural determinations were carried out on complexes **1b**, **2b** and **6b**. Crystals suitable for X-ray structural determinations were grown from layered $CH_2Cl_2$-pentane solutions (1:1); the molecular structures are shown in Figs. 1-3, with selected bond distances and angles collected in Table 1; see Fig. 4 for a numbered schematic for this Table.

All three structures are closely related; in each complex the M–N(pyridine) bond, ranging from 2.084(4) to 2.126(9) Å, is significantly shorter than the M–N(imino) bonds, which range from 2.207(5) to 2.272(11) Å. The formal double bond character of the imino linkages N7=C7 and N11=C11 are retained, with C=N distances in the range 1.267(18)–1.300(16) Å. The bond distances and angles compare well with those reported for similar 2,6-bis(imino)pyridyl iron(II) chloride complexes in the literature.[1] Regardless of the nature of the backbone or *ortho*-aryl substituents, the planes of the phenyl rings are orientated

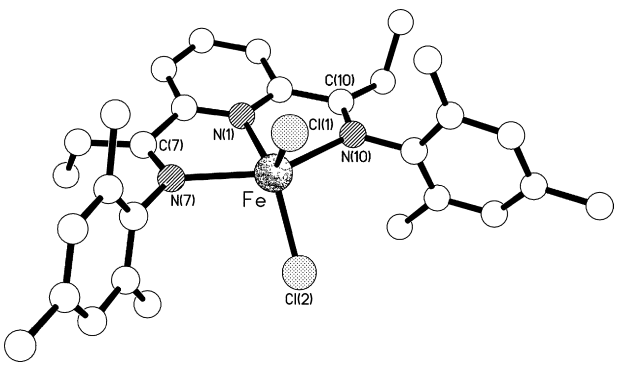


Fig. 1. The molecular structure of one (**I**) of the two independent complexes present in the crystals of **1b**.

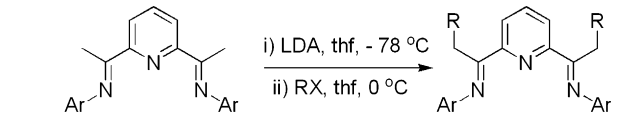


**I;** Ar = 2,4,6-trimethylphenyl (MES)
**II;** Ar = 2,6-diisopropylphenyl (DIPP)

i) LDA, thf, - 78 °C
ii) R'X, thf, 0 °C

| Ar | R | R' | |
|---|---|---|---|
| MES | Me | H | **1a** |
| MES | Me | Me | **2a** |
| MES | $CH_2Ph$ | H | **3a** |
| MES | $CH_2Ph$ | $CH_2Ph$ | **4a** |
| DIPP | Me | H | **5a** |
| DIPP | Me | Me | **6a** |

**1a-6a**

**1b** **2b** **3b**

**4b** **5b** **6b**

**7b**[1]

Scheme 1.

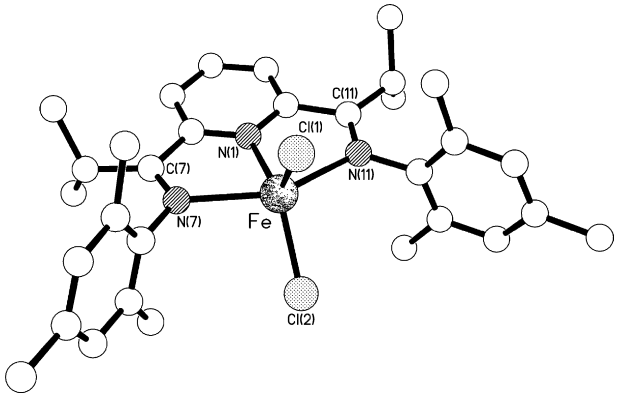


Fig. 2. The molecular structure of one (**I**) of the two independent complexes present in the crystals of **2b**.

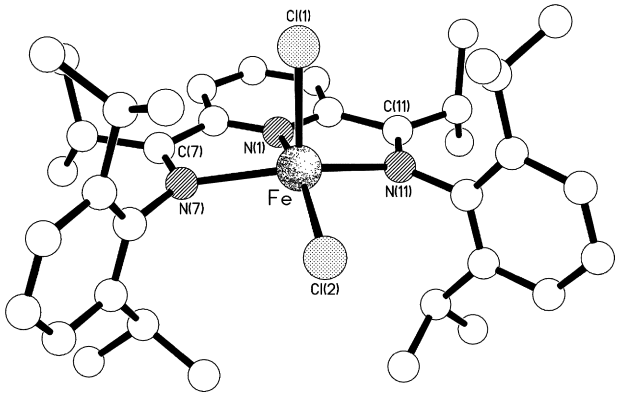


Fig. 3. Molecular structure of **6b**.

Table 1
Selected bond lengths (Å), angles (°) and derived parameters for **1b**, **2b** and **6b** (see Fig. 4 for a numbered schematic)

| | **1b** (R = Et, Ar = MES) | | **2b** (R = *i*-Pr, Ar = MES) | | **6b** [R = *i*-Pr, Ar = DIPP] |
|---|---|---|---|---|---|
| | Molecule **I** | Molecule **II** | Molecule **I** | Molecule **II** | |
| Fe–Cl1 | 2.305(4) | 2.300(5) | 2.291(3) | 2.296(2) | 2.3150(17) |
| Fe–Cl2 | 2.275(5) | 2.306(5) | 2.274(3) | 2.273(2) | 2.2446(16) |
| Fe–N1 | 2.126(9) | 2.105(11) | 2.108(6) | 2.091(5) | 2.084(4) |
| Fe–N7 | 2.232(11) | 2.260(10) | 2.264(6) | 2.207(5) | 2.224(4) |
| Fe–N11 | 2.272(11) | 2.240(11) | 2.266(6) | 2.213(5) | 2.233(5) |
| C7–N7 | 1.300(16) | 1.275(15) | 1.294(9) | 1.292(8) | 1.292(7) |
| C11–N11 | 1.282(18) | 1.267(18) | 1.276(10) | 1.294(9) | 1.283(8) |
| Cl1–Fe–Cl2 | 112.03(17) | 110.95(17) | 112.24(13) | 112.43(11) | 113.87(9) |
| Cl1–Fe–N1 | 118.9(3) | 120.1(3) | 117.9(2) | 108.2(2) | 90.68(14) |
| Cl1–Fe–N7 | 96.7(3) | 98.4(3) | 99.6(2) | 99.8(2) | 99.52(13) |
| Cl1–Fe–N11 | 100.6(3) | 100.2(3) | 97.8(2) | 102.9(2) | 99.92(13) |
| Cl2–Fe–N1 | 129.0(3) | 128.9(3) | 129.9(2) | 139.4(2) | 155.42(15) |
| Cl2–Fe–N7 | 101.8(3) | 101.3(3) | 99.0(2) | 99.17(15) | 101.94(12) |
| Cl2–Fe–N11 | 98.0(3) | 98.7(3) | 101.3(2) | 97.44(15) | 100.51(14) |
| N1–Fe–N7 | 74.0(4) | 72.7(4) | 73.3(2) | 73.7(2) | 73.62(16) |
| N1–Fe–N11 | 72.5(4) | 72.8(4) | 72.6(2) | 72.9(2) | 72.72(17) |
| N7–Fe–N11 | 146.5(4) | 145.5(4) | 145.9(2) | 144.0(2) | 141.04(18) |
| *A* (Å) [a] | 0.04 | 0.05 | 0.05 | 0.35 | 0.52 |
| *B* (°) [b] | 5.1 | 3.6 | 2.4 | 7.3 | 4.6 |
| *C* (°) [c] | 99 | 100 | 90 | 95 | 85 |
| *D* (°) [d] | 95 | 91 | 93 | 90 | 94 |

[a] **A** is the deviation of the iron centre from the $N_3$ plane. [b] **B** is the inclination of the $N_3$ and pyridyl ring planes. [c and d] **C** and **D** are the torsion angles about the N7–Ar and N11–Ar bonds respectively (ignoring the iron centre, using only the major occupancy orientations, and with an angle greater than 90° signifying a twist away from the Cl1 centre).

essentially orthogonal to the plane formed by the three nitrogen atoms ($N_3$ plane). The principal difference between complexes **1b** and **6b** is the deviation of the iron atom from the $N_3$ plane and the associated distortions from trigonal bipyramidal to square based pyramidal geometries.

The solid state structure of **1b** revealed the presence of two crystallographically independent molecules (**I** and **II**) in the asymmetric unit (molecule **I** is shown in Fig. 1, and molecule **II** in Fig. S2 in the supporting information). Though both molecules exhibit some disorder (see Figures S7 and S8) the major occupancy orientations are similar, having an r.m.s. fit of *ca.* 0.12 Å. The metal coordination geometry in both **I** and **II** is distorted trigonal bipyramidal with N(7) and N(10) in the axial positions [the iron atoms lie *ca.* 0.01 Å (molecule **I**) and 0.01 Å (molecule **II**) out of their respective {Cl(1),Cl(2),N(1)} planes]. Interestingly, in molecule **I**, and the major occupancy orientation of molecule **II**, the C(7) and C(10)-bound ethyl substituents adopt an anti configuration, giving both molecules approximate $C_2$ symmetry about the Fe–N(1) vector. (The C(10′) ethyl group of molecule **II** exhibits 60:40 disorder, with the minor orientation having the group flipped into a *syn* configuration cf. the C(7′) ethyl unit.)

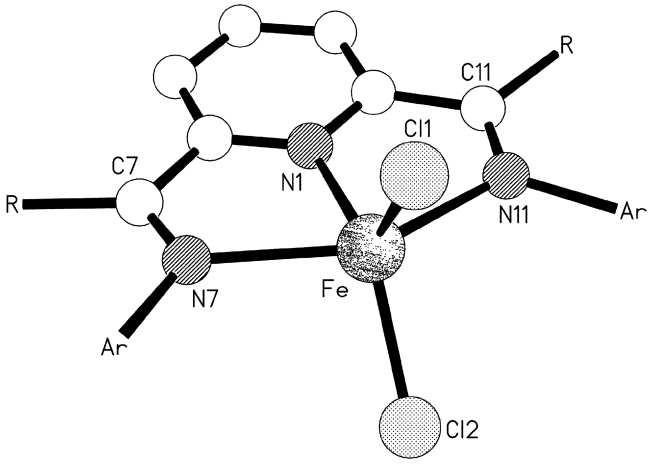


Fig. 4. Schematic representation of the metal coordination environment and ligand backbone in the structures of complexes **1b**, **2b** and **6b**.

As was seen for the structure of **1b**, X-ray analysis of a crystal of **2b** also revealed two independent molecules (**I** and **II**) in the asymmetric unit (molecule **I** is shown in Fig. 2, and molecule **II** in Figure S10 in the supporting information). Unlike the case seen for **1b**, however, here the two independent molecules are markedly different; whilst the iron centre in molecule **I** has a distorted trigonal bipyramidal coordination geometry, that in molecule **II** adopts a geometry intermediate between trigonal bipyramidal and square-based pyramidal (Figures S12 and S13, respectively). For molecule **I**, N(7) and N(11) occupy the axial positions, and the {Fe,Cl(1),Cl(2),N(1)} equatorial plane is coplanar to better than 0.01 Å. For molecule **II**, when viewed as square-based pyramidal, Cl(1′) occupies the apical site, and the iron centre lies *ca.* 0.61 Å out of the {Cl(2′),N(1′),N(7′),N(11′)} basal plane which is coplanar to within only *ca.* 0.18 Å. Both molecules have approximate $C_S$ symmetry about a plane that bisects the central pyridine ring and contains the iron and chlorine atoms.

In the solid state structure of **6b** (Fig. 3), the iron adopts a distorted square-based pyramidal coordination environment with Cl(1) in the apical position, and the iron lying *ca.* 0.48 Å out of the {Cl(2),N(1),N(7),N(11)} basal plane (which is coplanar to within *ca.* 0.03 Å). As was seen for both molecules in the structure of **2b**, here the complex has molecular $C_S$ symmetry about a plane that bisects the central pyridine ring and contains the iron and chlorine atoms.

The transition from trigonal bipyramidal to square-based pyramidal can be viewed as largely a twisting of the $FeCl_2$ unit along the N(1)···N(10/11) vector. In complexes **1b**(**I**), **1b**(**II**) and **2b**(**I**) the pyridyl and $N_3$ planes are near coplanar (inclined by *ca.* 5, 4 and 2° respectively), and bisect the Cl–Fe–Cl angle. In molecule **2b**(**II**) the pyridyl and $N_3$ planes are now slightly inclined (*ca.* 7°) and the $FeCl_2$ unit is slightly twisted along the N(7′)···N(11′) vector such that Cl(2′) is much closer to the $N_3$ plane than Cl(1′) (*ca.* 0.81 and 2.62 Å respectively). For complex **6b** this twisting has proceeded further with Cl(2) and Cl(1) now *ca.* 0.12 and 2.77 Å, respectively out of the $N_3$ plane. The reasons for these changes of geometry are far from clear. Since the altered groups are distal to the iron and chlorine atoms a steric argument is unconvincing; equally tenuous would be an argument based on electronic differences between ethyl and isopropyl, and between mesityl and diisopropylphenyl. What is clear is that square-based pyramidal and trigonal bipyramidal geometries lie on a very shallow energy surface for these Fe(II) complexes.

### 3.3. Ethylene polymerization studies

All of the complexes are active for ethylene polymerisation upon treatment with methylaluminoxane (MAO), affording highly linear polyethylenes with broad molecular weight distributions (Table 2), typical of iron ethylene polymerisation catalysts supported by bis(imino)pyridine ligands.[1] Changing the aryl ring attached to imine nitrogen from 2,4,6-trimethylphenyl to 2,6-diisopropylphenyl has a marked effect on catalyst behaviour. Catalysts bearing 2,4,6-trimethylphenyl substituents (**1b**–**4b** and **7b**) are considerably more productive than their 2,6-diisopropylphenyl bearing relatives (**5b** and **6b**). This is attributed to less congested active sites for 2,4,6-trimethylphenyl derivatives resulting in increased propagation rates. A comparison of the polyethylene products obtained using **2b** and **6b** reveal an increase in the molecular weight for the 2,6-diisopropylphenyl derivative, an effect that is less marked for the ethyl pair **1b** and **5b**.

Replacing one of the ketimine methyl protons of **7b** with alkyl substituents (**1b** and **3b**) has only a minor effect on catalyst performance. Virtually identical activities are obtained to benchmark catalyst **7b** with only minor differences in the molecular weights of the resultant polyethylenes. Introducing a second methyl to give isopropyl backbone substituents leads to a more substantial increase in $M_{pk}$ (82,000 for **2b** cf. 47,000 for **7b**), while for the dibenzyl derivative a much higher molecular weight is seen ($M_{pk}$ 422,000). Increasing the size of the imine carbon substituent is expected to result in a greater rotational barrier for the *N*-aryl rings (as indicated by NMR studies on ligands **1a**–**6a**). Thus, the steric interaction between the large dibenzylmethine and the aryl substituents in **4b** may effectively 'lock' the 2,4,6-trimethylphenyl ring perpendicular to the $N_3$ coordination plane. This places the *ortho* aryl substituents above and below the metal centre where they are anticipated to be most effective at reducing the rate of chain transfer processes. The imine carbon substituents in **1b**–**3b** appear to be insufficiently bulky for such purposes. As might be expected, the larger 2,6-diisopropylphenyl rings can be 'locked' with smaller backbone groups, such that replacing ethyl (**5b**) with isopropyl (**6b**) substituents leads to a more marked increase in polymer molecular weight (**5b**; $M_{pk}$ 26 000, **6b**; $M_{pk}$ 263,000) whereas the same modification to the ligand backbone had less impact on the polymer molecular weight obtained using mesityl bearing catalysts (**1b** and **2b**).

Significantly, it has been noted in earlier studies [1] that bulky aryl substituents, e.g. 2,6-diisopropylphenyl, attached to the imine nitrogen donors are required to afford high molecular weight products. However, this is accompanied by a substantial penalty on catalyst productivity compared with, for example, smaller aryl substituents such as 2,4,6-trimethylphenyl. The findings reported here show that molecular weight can be dramatically raised by increasing the steric hindrance at the ketimine carbon site, in combination with *N*-2,4,6-trimethylphenyl donors, without any significant sacrifice over catalyst productivity.

Table 2
Results of ethylene polymerisation runs using pre-catalysts **1b**–**7b**[a]

| Run | Pre-cat. | Yield (g) | Activity (g/mmol bar h) | $M_n$[b] | $M_w/M_n$[b] | $M_{pk}$[b] |
|---|---|---|---|---|---|---|
| 1 | **1b** | 34.2 | 17,100 | 10,000 | 16.5 | 35,000 |
| 2 | **2b** | 35.6 | 17,800 | 12,000 | 38.0 | 82,000 |
| 3 | **3b** | 32.5 | 16,250 | 6,500 | 30.4 | 26,000 |
| 4 | **4b** | 33.6 | 16,800 | 15,000 | 31.2 | 422,000 |
| 5 | **5b** | 6.3 | 3,160 | 14,000 | 25.4 | 26,000 |
| 6 | **6b** | 6.0 | 3,000 | 24,000 | 22.8 | 263,000 |
| 7 | **7b** | 32.1 | 16,050 | 9,400 | 22.0 | 47,000 |

[a] Isobutane solvent, 4 bar ethylene, catalyst loading 0.5 μmol, 100 equiv. MAO activator, *i*-$Bu_3Al$ scavenger, 50 °C, reaction time 1 h.
[b] Determined by GPC at 135 °C.

## 4. Conclusions

A straightforward synthetic strategy, based on deprotonation and alkylation, has been employed to derivatise 2,6-bis(imino)pyridyl ligands at the α-imino carbon position. For ligands bearing bulky backbone substituents, slow rotation of the aryl rings occurs on the NMR time scale at room temperature due to steric interactions between the *ortho*-aryl and α-imino carbon substituents. All of the pre-catalysts **1b**–**6b** are highly active ethylene polymerisation catalysts upon treatment with MAO. Increasing the size of the backbone position is shown to increase the molecular weight of the resultant polyethylene due to an increase in the effective steric protection of the metal centre, but without lowering the catalyst productivity.

## Acknowledgements

The authors are grateful to BP Chemicals, Ltd. (now Ineos Technologies) for financial support and to Crompton Co. for the donation of MAO. Drs. J. Boyle and G. Audley are thanked for NMR and GPC measurements, respectively.

## Appendix A. Supplementary data

Supplementary data associated with this article can be found, in the online version, at doi:10.1016/j.molcata.2006.10.028.

## References

[1] G.J.P. Britovsek, M. Bruce, V.C. Gibson, B.S. Kimberley, P.J. Maddox, S. Mastroianni, S.J. McTavish, C. Redshaw, G.A. Solan, S. Strömberg, A.J.P. White, D.J.J. Williams, J. Am. Chem. Soc. 121 (38) (1999) 8728–8740.
[2] G.J.P. Britovsek, V.C. Gibson, B.S. Kimberley, P.J. Maddox, S.J. McTavish, G.A. Solan, A.J.P. White, D.J.J. Williams, Chem. Commun. (7) (1998) 849–850.
[3] B.L. Small, M. Brookhart, A.M.A. Bennett, J. Am. Chem. Soc. 120 (16) (1998) 4049–4050.
[4] Y. Chen, R. Chen, C. Qian, X. Dong, J. Sun, Organometallics 22 (21) (2003) 4312–4321.
[5] Y.F. Chen, C.T. Qian, J. Sun, Organometallics 22 (6) (2003) 1231–1236.
[6] G.J.P. Britovsek, V.C. Gibson, B.S. Kimberley, S. Mastroianni, C. Redshaw, G.A. Solan, A.J.P. White, D.J.J. Williams, Dalton Trans. (10) (2001) 1639–1644.
[7] A.S. Abu-Surrah, K. Lappalainen, U. Piironen, P. Lehmus, T. Repo, M. Leskela, J. Organomet. Chem. 648 (1–2) (2002) 55–61.
[8] G.J.P. Britovsek, S. Mastroianni, G.A. Solan, S.P.D. Baugh, C. Redshaw, V.C. Gibson, A.J.P. White, D.J.J. Williams, M.R.J. Elsegood, Chem. Eur. J. 6 (12) (2000) 2221–2231.
[9] M.E. Blum, C. Folli, M. Döring, J. Mol. Catal. A: Chem. 212 (1–2) (2004) 13–18.
[10] C. Amort, M. Malaun, A. Krajete, H. Kopacka, K. Wurst, M. Christ, D. Lilge, M.O. Kristen, B. Bildstein, Appl. Organomet. Chem. 16 (9) (2002) 505–516.
[11] Z. Ma, H. Wang, J. Qiu, D. Xu, Y. Hu, Macromol. Rapid Commun. 22 (15) (2001) 1280–1283.
[12] A.S. Ionkin, W.J. Marshall, D.J. Adelman, B.B. Fones, B.M. Fish, M.F. Schiffhauer, Organometallics 25 (2006) 2978–2992.
[13] V.C. Gibson, N.J. Long, P.J. Oxford, A.J.P. White, D.J. Williams, Organometallics 25 (2006) 1932–1939.
[14] A.M.A. Bennett, (E.I. Du Pont de Nemours and Co., USA) WO9827124, 1998. [CAN 129:122973].
[15] T.M. Smit, A.K. Tomov, V.C. Gibson, A.J.P. White, D.J. Williams, Inorg. Chem. 43 (21) (2004) 6511–6512.
[16] F.A.R. Kaul, G.T. Puchta, H. Schneider, F. Bielert, D. Mihalios, W.A. Herrmann, Organometallics 21 (2002) 74–82.
[17] K. Nomura, W. Sidokmai, Y. Imanishi, Bull. Chem. Soc. Jpn. 73 (3) (2000) 599–605.
[18] G.J.P. Britovsek, V.C. Gibson, O.D. Hoarau, S.K. Spitzmesser, A.J.P. White, D.J.J. Williams, Inorg. Chem. 42 (11) (2003) 3454–3465.
[19] G.J.P. Britovsek, V.C. Gibson, S. Mastroianni, D.C.H. Oakes, C. Redshaw, G.A. Solan, A.J.P. White, D.J.J. Williams, Eur. J. Inorg. Chem. (2) (2001) 431–437.
[20] S. Al-Benna, M.J. Sarsfield, M. Thornton-Pett, D.L. Ormsby, P.J. Maddox, P. Bres, M. Bochmann, Dalton Trans. (23) (2000) 4247–4257.
[21] S.J. McTavish, M.J. Payne, (BP Chemicals Ltd, UK), WO2001023396, 2001. [CAN 134:281263].
[22] D.F. Evans, J. Chem. Soc. (1959) 2003–2005.
[23] M. Fieser, Reagents for Organic Synthesis, Wiley-Interscience, Chichester, 1979.